

## Fe<sup>3+</sup> Selective Pyrimidine Based Chromogenic and Fluorogenic Chemosensor

Prashant Patil<sup>1,\*</sup>, Swapnil Shinde<sup>1</sup> and Suban Sahoo<sup>2</sup>

<sup>1</sup>Department of Chemistry, S. S. V. P. S's L. K. Dr. P. R. Ghogrey Science College, Deopur, Dhule (M.S.) 424005, India

<sup>2</sup>Department of Chemistry, Sardar Vallabhbhai National Institute of Technology, Surat, Gujarat 395007, India

(\*Corresponding author's e-mail: prashantchem5@gmail.com)

Received: 1 June 2022, Revised: 18 July 2022, Accepted: 28 July 2022, Published: 9 November 2022

### Abstract

By using UV-Visible and fluorescence measurements, a new chemosensor N-(pyrimidin-2-yl) thiophene-2-carboxamide (PTC) was introduced for the discriminating and responsive detection of Fe<sup>3+</sup> in aqueous methanolic medium. Since the PTC-Fe<sup>3+</sup> complexation occurred in 1:1 binding stoichiometry, the receptor PTC preferentially revealed a charge transfer band between 310 to 475 nm in the UV-Vis technique, with the absorption peak at 351 nm. Furthermore, the fluorescence technique, which dampened PTC's fluorescence emission band at 325 nm, showed similar selectivity. The Stern-Volmer graphic shows that fluorescence quenching occurs in a static manner. The series of examined metal ions (Na<sup>+</sup>, K<sup>+</sup>, Li<sup>+</sup>, Cs<sup>+</sup>, Fe<sup>2+</sup>, Ni<sup>2+</sup>, Sr<sup>2+</sup>, Cu<sup>2+</sup>, Cd<sup>2+</sup>, Pb<sup>2+</sup>, Co<sup>2+</sup>, Hg<sup>2+</sup>, Ba<sup>2+</sup>, Mg<sup>2+</sup>, Mn<sup>2+</sup>, Ca<sup>2+</sup>, Zn<sup>2+</sup>, Cr<sup>3+</sup>, Ag<sup>+</sup> and Al<sup>3+</sup>) failed to perturb the UV-Vis and fluorescence of PTC. With PTC, the concentration of Fe<sup>3+</sup> can be detected down to 2.03 and 1.24 μM by UV-Vis and fluorescence methods, respectively.

**Keywords:** Chemosensor, Pyrimidine based chromogenic, UV-Vis, Fluorescence, Fe<sup>3+</sup>

### Introduction

The advancement of chromogenic and fluorogenic chemosensors for the recognition of bioactive and venomous species from metal ions, anions, amino acids, explosives, pesticides etc. have ensnared far-reaching interest in the area of analytical chemistry, environmental and life sciences for their simplicity, low cost and high sensitivity [1-5]. In many biological and environmental processes, metal ions play a decisive role. However, the unnecessary consumption and deposition of metal ions in living body is detrimental although some essential metal ions in optimal quantity is required to maintain normal health [6-8]. The Fe<sup>3+</sup> is an essential metal ion that plays an important role in a variety of biological activities at the cellular level. Various enzymes make use of Fe<sup>3+</sup> as a catalyst for RNA and DNA synthesis, electron transfer and oxygen metabolism [9,10]. In humans, however, iron deficiency (hypoferremia) can lead to hemochromatosis, anemia, liver damage, diabetes, and cancer. [11,12], while excess of iron (hyperferremia) can induce a variety of diseases such as Huntington's, Alzheimer's, Parkinson's disease [13,14]. As a result, there is need of rapid, sensitive and convenient analytical method for the on-site detection of Fe<sup>3+</sup> in a variety of ecological as well as biological samples.

The optical based i.e. colorimetric and fluorescent chemosensors can be designed conveniently and applied for the rapid on-site recognition of target metal ions. The chemosensor possess binding sites that selectively recognize the target metal ions upon complexation and concomitantly showed a distinct color or spectral changes in UV-Vis/fluorescence that can be used for the detection and quantification. Over the past 2 decades, several chemosensors were reported for the detection of Fe<sup>3+</sup>. Most of the them involves use of complex starting material and multistep synthesis of chemosensor [15]. However, there is a need of novel chemosensors that can be applied to sense Fe<sup>3+</sup> both by UV-Vis and fluorescence method from aqueous medium. As a part of our ongoing research to develop cost-effective and easy-to-prepare optical chemosensors [16-19], a new chemosensor N-(pyrimidin-2-yl)thiophene-2-carboxamide (PTC) was introduced for the detection of Fe<sup>3+</sup>. The donor atoms like O, S and N in PTC makes this easy-to-prepare receptor an ideal candidate to develop as metal ions sensor. The PTC's ability to sense metal ions was investigated using UV-Vis and fluorescence techniques.

## Materials and methods

### Materials

All of the reagents used in the synthesis of PTC and the perchlorate salts of metal ions were acquired from Sigma Aldrich Ltd. and are of analytical grade. For all sensing studies, spectroscopic grade solvents were utilized. PTC stock solution ( $1.0 \times 10^{-3}$  M) was made in MeOH, while metal perchlorates stock solution ( $1.0 \times 10^{-2}$  M) was made in water. After adequate dilution, all of these solutions were employed for sensing studies. Analytical thin layer chromatography (TLC) was used to monitor the reaction's progress using pre-coated silica gel 60 F254 (Merck) laid out on alumina plates.

All UV-Vis spectrum analysis was done with a Perkin Elmer U-3900 spectrophotometer and a quartz cuvette with a path length of 1 cm. Fluorescence spectral analysis was performed using a Fluoromax-4 spectrofluorometer (HORIBA Jobin Yvon Co., France).

### Analytical method of synthesis of PTC

In 100 mL round bottom flask, 2-aminopyrimidine (0.95 g, 0.01 moles) was dissolved in 10 mL dichloromethane. To this solution, pyridine (0.8 mL, 0.01 moles) was added and the resulting reaction mixture was stirred at 0 °C for 10 min. To this stirred solution, thiophene-2-carbonyl chloride (1.042 mL, 0.01 moles) was added drop wise. The resulting reaction mass was stirred for overnight. Once the reaction was completed (TLC; hexane/EtOAc; 8:2), 15 mL water was added to the reaction mixture and the product was extracted with dichloromethane ( $2 \times 100$  mL) and dried over  $\text{Na}_2\text{SO}_4$ , followed by filtered on funnel and recrystallized from ethanol get pure product [20].

### Characterization of PTC

PTC's FT-IR spectrum was recorded as KBr pellets on a Bruker ALPHA FT-IR spectrometer. On a Varian (Mercury Vx) SWBB Multinuclear probe spectrometer with tetramethyl silane (TMS) as an internal standard,  $^1\text{H}$  NMR spectra of PTC in  $\text{CH}_3\text{OH}-d_4$  at 300 MHz and  $^{13}\text{C}$  NMR spectra at 75 MHz were acquired. The chemical shifts are measured in parts per million (ppm).

FT-IR (KBr pellet,  $\text{cm}^{-1}$ ): 3334 ( $\nu_{\text{N-H}}$ ), 1673 ( $\nu_{\text{C=O}}$ ), 1592 ( $\nu_{\text{C=C Ar}}$ ), 1433-1285 (for pyridine  $\nu_{\text{C-C}}$ );  $^1\text{H}$  NMR (300 MHz,  $\text{CH}_3\text{OH}-d_4$ ,  $\delta$  ppm): 7.17 (dd,  $J = 4.1$  Hz and  $J = 1.3$  Hz, 1H), 7.19 (dd,  $J = 5.5$  Hz and  $J = 2.0$  Hz, 1H), 7.78 (d,  $J = 4.5$  Hz, 1H), 7.96 (dd,  $J = 4.1$  Hz and  $J = 1.3$  Hz, 1H), 8.65 (dd,  $J = 8.5$  Hz, 2H), 10.71 (s, 1H);  $^{13}\text{C}$  NMR (75 MHz,  $\text{CH}_3\text{OH}-d_4$ ,  $\delta$  ppm): 108.9, 119.5, 121.9, 124.3, 130.7, 140.0, 149.6, 150.0, 152.6; Mass (HRMS): 206 ( $M + 1$ ), 228 ( $M + \text{Na}$ ).

## Results and discussion

By reacting equimolar amounts of 2-aminopyrimidine and thiophene-2-carbonyl chloride in one step, the receptor PTC was produced (Figure 1) [20]. The structure of PTC was established by diverse spectral data (Figures S1 - S4). Then, the metal ions recognition ability of PTC was explored by both UV-Vis and fluorescence methods.

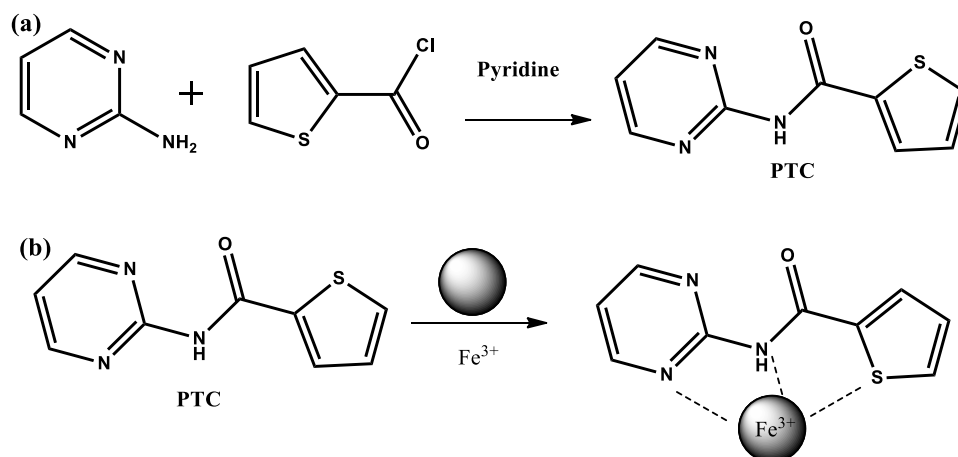


**Figure 1** (a) Synthesis of the receptor PTC and (b) the possible coordination mode between PTC and  $\text{Fe}^{3+}$ .

The naked-eye detectable color change experiment was executed to scrutinize the cation detection ability of PTC. In this method, the solution of PTC (2 mL,  $5 \times 10^{-5}$  M) in MeOH was treated with 300  $\mu$ L ( $1 \times 10^{-2}$  M, in H<sub>2</sub>O) of a variety of metal ions (Na<sup>+</sup>, K<sup>+</sup>, Li<sup>+</sup>, Cs<sup>+</sup>, Fe<sup>2+</sup>, Fe<sup>3+</sup>, Ni<sup>2+</sup>, Sr<sup>2+</sup>, Cu<sup>2+</sup>, Cd<sup>2+</sup>, Pb<sup>2+</sup>, Co<sup>2+</sup>, Hg<sup>2+</sup>, Ba<sup>2+</sup>, Mg<sup>2+</sup>, Mn<sup>2+</sup>, Ca<sup>2+</sup>, Zn<sup>2+</sup>, Cr<sup>3+</sup>, Ag<sup>+</sup> and Al<sup>3+</sup>). As shown in **Figure 2(a)**, the colorless solution of PTC instantaneously turned to yellow-brown color selectively in existence of Fe<sup>3+</sup>. The color change supported the ability of PTC to sense Fe<sup>3+</sup> selectively over the other examined metal ions. Further, the UV-Vis spectrum of PTC (2 mL,  $5 \times 10^{-5}$  M) in MeOH were traced in the existence of diverse metal cations (40  $\mu$ L,  $1 \times 10^{-2}$  M, in H<sub>2</sub>O) (**Figure 2(b)**). The receptor PTC shows a strong absorption band at 272 nm due to  $\pi \rightarrow \pi^*$  transition. With the addition of Fe<sup>3+</sup>, the band at 272 nm was blue-shifted by  $\sim 10$  nm and a new band appeared at 351 nm with a long-tail up to  $\sim 475$  nm because of the charge-transfer occurred among the Fe<sup>3+</sup> and the receptor PTC upon formation of a novel complex species Fe<sup>3+</sup>-PTC in solution. Other metal cations botched to perturb the UV-Vis profile of PTC, except addition of Ni<sup>2+</sup> shift the absorption band of PTC from 272 to 288 nm.

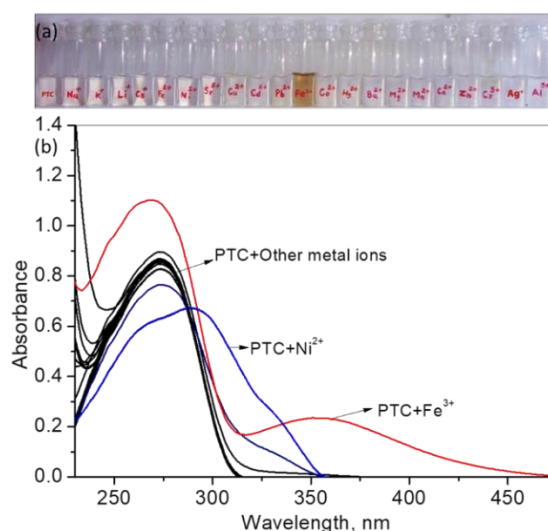


**Figure 2** (a) PTC color change visible to the naked eye (2 mL,  $5 \times 10^{-5}$  M, in MeOH) in the existence of diverse metal cations (300  $\mu$ L,  $1 \times 10^{-2}$  M, in H<sub>2</sub>O); (b) UV-Vis spectral changes of PTC (2 mL,  $5 \times 10^{-5}$  M, in MeOH) on adding up of 5 equivalents of diverse metal cations (40  $\mu$ L,  $1 \times 10^{-2}$  M, in water).

The UV-Vis spectral response of PTC in the existence of Fe<sup>3+</sup> prompted us to examine the competitive experiment, where the absorption spectra of the solution containing PTC (2 mL,  $5 \times 10^{-5}$  M in MeOH) were recorded by adding 40  $\mu$ L of Fe<sup>3+</sup> ions ( $1.0 \times 10^{-2}$  M, in H<sub>2</sub>O) and equimolar amount of other competitive metal ions (40  $\mu$ L,  $1 \times 10^{-2}$  M, in H<sub>2</sub>O). The bar illustration of the spectral transformation examined throughout the interference experiment designates that the Fe<sup>3+</sup> selectivity of PTC was not obstructed by the subsistence of the interfering metal ions including Ni<sup>2+</sup> (**Figure 3**). These findings backed up PTC's remarkable selectivity for Fe<sup>3+</sup> over the other metal ions studied.

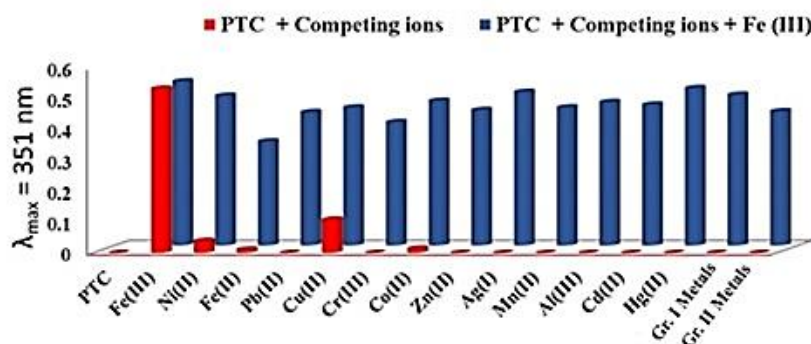


**Figure 3** Competitive responses of PTC (2 mL,  $5 \times 10^{-5}$  M, in MeOH) in the existence of Fe<sup>3+</sup> (40  $\mu$ L,  $1 \times 10^{-2}$  M, in H<sub>2</sub>O) and at equimolar quantities of other interfering metal cations.

The UV-Vis absorption titration of PTC with the selective  $\text{Fe}^{3+}$  ion was performed to examine the sensitivity. The receptor band at 272 nm was increased and red-shifted after adding incremental amounts of  $\text{Fe}^{3+}$  to the PTC solution, while a new charge transfer band at 351 nm appeared at the same time (**Figure 4**). From the titration results, the binding constant of  $4 \times 10^4 \text{ M}^{-1}$  was determined for the new complex species  $\text{Fe}^{3+}$ -PTC in solution by applying the Benesi-Hildebrand equation (**Figure S5**). In addition, the LOQ (limit of quantification) and LOD (limit of detection) respectively of 6.16 and 2.03  $\mu\text{M}$  for  $\text{Fe}^{3+}$  were determined by employing the IUPAC permitted equation,  $\text{LOD} = 3\sigma/\text{slope}$  of the calibration curve (**Figure S6**), where the ' $\sigma$ ' denotes the blank sample's standard deviation.

The Job's method was employed to analyze the binding stoichiometry between PTC and  $\text{Fe}^{3+}$  [21]. The Job's graphic validated the 1:1 stoichiometry of complexation between PTC and  $\text{Fe}^{3+}$  (**Figure S7**). Additionally, direct authentication for the complex formation in 1:1 stoichiometry was supported from the mass spectrum of PTC recorded in existence of 1 equivalent  $\text{Fe}^{3+}$ . The mass peak of pure PTC was observed at  $m/z = 228.0$  (**Figure S2**) ( $\text{PTC} + \text{Na}$ ), whereas with the addition of 1 equivalent of  $\text{Fe}^{3+}$  to PTC, a new mass peak obtained at  $m/z = 548.9$  assigned for the complex  $(\text{PTC}) + [\text{Fe}(\text{ClO}_4)_2]^+ + 5\text{H}_2\text{O}$  (**Figure S8**).

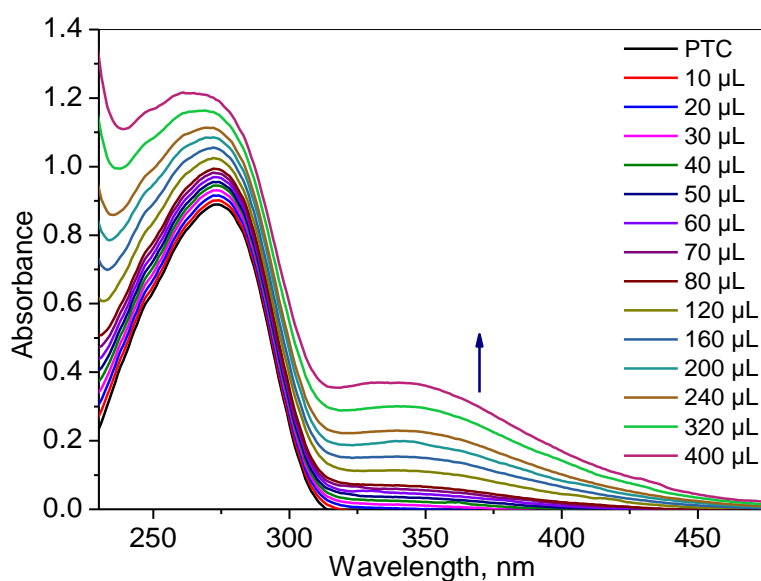


**Figure 4** PTC (2 mL,  $5 \times 10^{-5} \text{ M}$  in MeOH) absorption spectrum changes as  $\text{Fe}^{3+}$  ions (0 - 400  $\mu\text{L}$ ,  $1 \times 10^{-3} \text{ M}$ , in water) were added incrementally.

The fluorescence method was also applied to scrutinize the capability of PTC to sense metal ions. Addition of 40  $\mu\text{L}$  of  $\text{Fe}^{3+}$  ions ( $1 \times 10^{-2} \text{ M}$ , in  $\text{H}_2\text{O}$ ) to the PTC solution (2 mL,  $5 \times 10^{-5} \text{ M}$ , in MeOH) fallout in a selective fluorescence quenching (**Figure 5**). Conversely, with the addition of metal ions like  $\text{Na}^+$ ,  $\text{K}^+$ ,  $\text{Li}^+$ ,  $\text{Cs}^+$ ,  $\text{Fe}^{2+}$ ,  $\text{Ni}^{2+}$ ,  $\text{Sr}^{2+}$ ,  $\text{Cu}^{2+}$ ,  $\text{Cd}^{2+}$ ,  $\text{Pb}^{2+}$ ,  $\text{Co}^{2+}$ ,  $\text{Hg}^{2+}$ ,  $\text{Ba}^{2+}$ ,  $\text{Mg}^{2+}$ ,  $\text{Mn}^{2+}$ ,  $\text{Ca}^{2+}$ ,  $\text{Zn}^{2+}$ ,  $\text{Cr}^{3+}$ ,  $\text{Ag}^+$  and  $\text{Al}^{3+}$ , the fluorescence intensity of PTC at 325 nm showed very negligible changes. Fluorescence investigations were next used to investigate PTC's  $\text{Fe}^{3+}$  sensing abilities in the presence of potentially probing metal cations in a competitive media. (**Figure 6**). The addition of 2 equivalents. of  $\text{Fe}^{3+}$  to PTC solution in MeOH, together with 2 equivalents. of other interfering metal ions, had no effect on  $\text{Fe}^{3+}$ 's fluorescence quenching capabilities. As a result of the selectivity investigations, the receptor PTC can be designed as a  $\text{Fe}^{3+}$  fluorescence turn-off sensor.

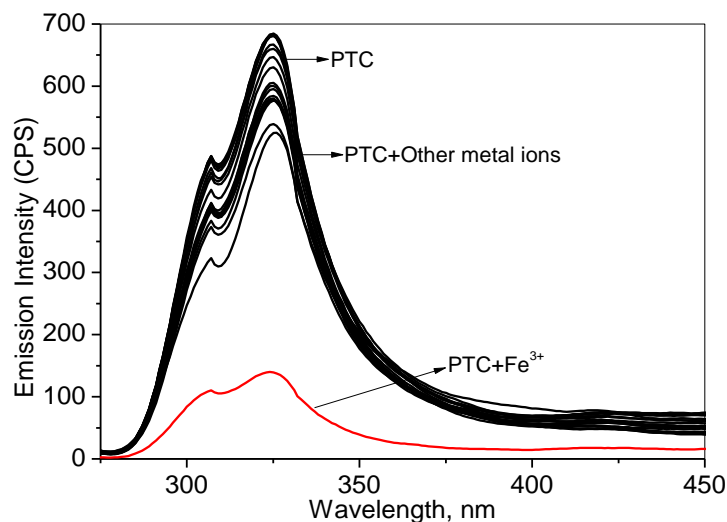


**Figure 5** Fluorescence spectral ( $\lambda_{\text{ex}} = 275 \text{ nm}$ ) changes of PTC ( $5 \times 10^{-5} \text{ M}$ , in MeOH) when 5 equivalents of a variety of metal ions are added ( $1 \times 10^{-2} \text{ M}$ , in water).

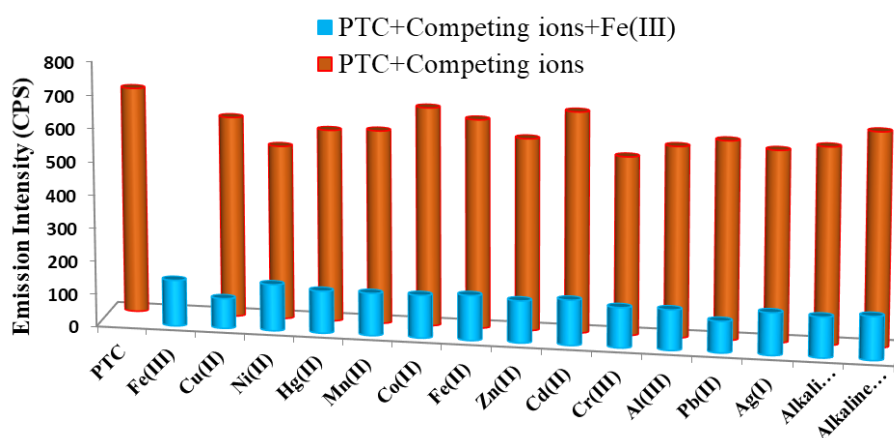


**Figure 6** Competitive responses of PTC in the company of  $\text{Fe}^{3+}$  and other interfering metal ions.

The titration of PTC (2 mL,  $5 \times 10^{-5} \text{ M}$ , in MeOH) using fluorescence with  $\text{Fe}^{3+}$  was carried out by the use of the subsequent addition of incremental concentrations of  $\text{Fe}^{3+}$  ( $1 \times 10^{-3} \text{ M}$ , 0 - 400  $\mu\text{L}$ , in water). The intensity of fluorescence for PTC was gradually decreased at 325 nm (**Figure 7**). The paramagnetic behavior of  $\text{Fe}^{3+}$  is responsible for quenching of fluorescence [22-24]. Using the fluorescence titration, the corresponding quantification and detection limits of 3.75 and 1.24  $\mu\text{M}$  were estimated for  $\text{Fe}^{3+}$  (**Figure S9**). Also, the association constant of PTC with  $\text{Fe}^{3+}$  was evaluated by using the Benesi-Hildebrand equation from the data obtained by performing fluorescence titration (**Figure S10**). The  $\text{Fe}^{3+}$  binding affinity of PTC was revealed to be  $2.25 \times 10^5 \text{ M}^{-1}$ . Job's Method was used to evaluate the binding stoichiometry of PTC with  $\text{Fe}^{3+}$  using the fluorescence method. The Job's plot confirms the establishment of a 1:1 binding stoichiometry complex between PTC and  $\text{Fe}^{3+}$  (**Figure S11**).

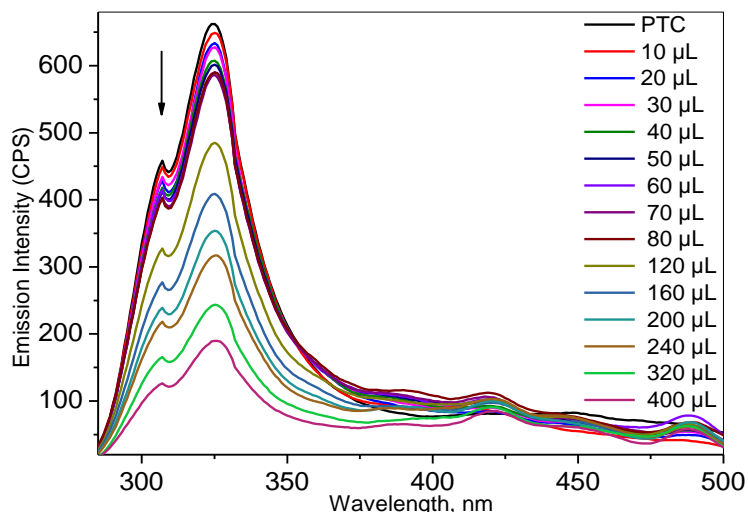


**Figure 7** Fluorescence spectral changes of sensor PTC (2 mL,  $5 \times 10^{-5}$  M, in MeOH) upon addition of 0 - 10 equivalents of  $\text{Fe}^{3+}$  (0 - 400  $\mu\text{L}$ ,  $1 \times 10^{-3}$  M, in  $\text{H}_2\text{O}$ ) at  $\lambda_{\text{ex}} = 275$  nm.

The Stern-Volmer Eq. (1) can mathematically express the quenching process, which permits us to decide the quenching type. The quenching type is static if the linearity is observed in Stern-Volmer plot.

$$F_0/F = 1 + k_q\tau_0[Q] = 1 + K_{sv}[Q] \quad (1)$$

Where  $F_0$  is the fluorescence intensity in the absence of the quencher and  $F$  is the fluorescence intensity in the presence of the quencher,  $k_q$  is the bimolecular quenching constant,  $\tau_0$  stands for the lifetime of the fluorescence in the absence of the quencher,  $[Q]$  is the quencher concentration, and  $K_{sv}$  is the Stern-Volmer quenching constant. In the existence of a quencher, the fluorescence intensity is quenched from  $F_0$  to  $F$ . As a result, the quencher concentration  $[Q]$  is proportional to the ratio  $(F_0/F)$  in a direct relationship. According to Eq. (1), the Stern-Volmer plot of  $F_0/F$  versus  $[Q]$  illustrate a linear graph with a slope of  $K_{sv}$  (**Figure 8**). The linearity of Stern-Volmer plot designates the static quenching for the PTC.  $\text{Fe}^{3+}$  coordination [25]. These results also confirm the development of a new complex among the receptor PTC and the  $\text{Fe}^{3+}$  ions resulted the fluorescence quenching.

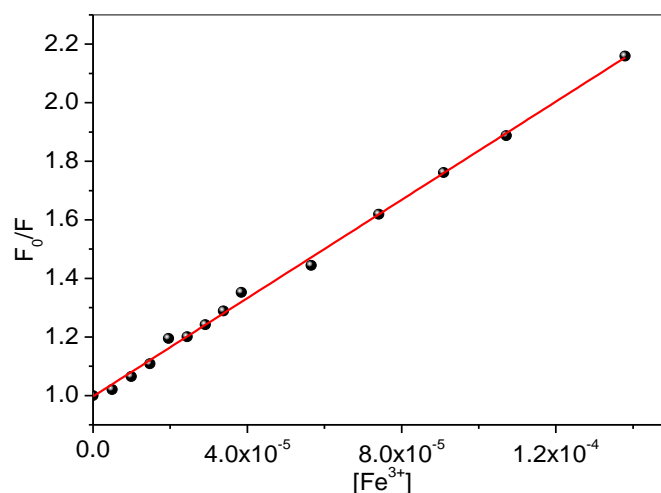


**Figure 8** Stern-Volmer plot for  $\text{Fe}^{3+}$  with receptor PTC.

## Conclusions

To conclude, a new pyrimidine-based chemosensor, PTC, was developed for the selective detection of Fe<sup>3+</sup> in aqueous medium using colorimetric, UV-Visible, and fluorescence techniques. The PTC receptor formed a 1:1 stoichiometric complex with Fe<sup>3+</sup>, resulting in the formation of a new charge transfer band at 351 nm and fluorescence quenching at 325 nm. Among the other metal ions tested, the receptor has a high preference for Fe<sup>3+</sup>. With PTC, the concentration of Fe<sup>3+</sup> can be detected down to 2.03 and 1.24 μM by means of the UV-Vis and fluorescence method, respectively. Based on the results, we believe the newer pyrimidine based chemosensors will be designed because of the low cost, simplicity of preparation and high selectivity towards metal ions.

## Acknowledgements

The author Dr. Prashant Patil is thankful to the Principal, S. S. V. P. S's L. K. Dr. P. R. Ghogrey Science College, Dhule, India and to the Director, SVNIT for providing necessary research facilities and infrastructure.

## References

- [1] CD Geddes and JR Lakowicz. *Advanced concepts in fluorescence sensing part A: Small molecule sensing*. Springer, New York, 2005.
- [2] APD Silva, HQ Gunaratne, N Gunnlaugsson, AJ M Huxley, CP McCoy, JT Rademacher and TE Rice. Signaling recognition events with fluorescent sensors and switches. *Chem. Rev.* 1997; **97**, 1515-66.
- [3] APD Silva, DB Fox, AJM Huxley and TS Moody. Combining luminescence, coordination and electron transfer for signaling purposes. *Coord. Chem. Rev.* 2000; **205**, 41-57.
- [4] C Bargossi, MC Fiorini, M Montalti, L Prodi and N Zaccheroni. Recent developments in transition metal ion detection by luminescent chemosensors. *Coord. Chem. Rev.* 2000; **208**, 17-32.
- [5] R Martinez-Manez and F Sancenon. Fluorogenic and chromogenic chemosensors and reagents for anions. *Chem. Rev.* 2003; **103**, 4419-76.
- [6] HLJ Fan and X Peng. Colorimetric and fluorescent probes for the optical detection of palladium ions. *Chem. Soc. Rev.* 2013; **42**, 7943-62.
- [7] H Dai, Y Yan, Y Guo, L Fan, Z Che and H Xu. A selective and sensitive "Turn-on" fluorescent chemosensor for recognition of Hg<sup>2+</sup> ions in water. *Chem. Eur. J.* 2012; **18**, 11188.
- [8] PG Georgopoulos, A Roy, MJ Yonone-Lioy, RE Opiekun and PJ Lioy. Environmental copper: Its dynamics and human exposure issues. *J. Toxicol. Environ. Health, Part B* 2001; **4**, 341-94.
- [9] SK Sahoo, D Sharma, RK Bera, G Crisponi and JF Callan. Iron (III) selective molecular and supramolecular fluorescent probes. *Chem. Soc. Rev.* 2012; **41**, 7195-227.
- [10] RH Crabtree. Metal ions at work. *Science* 1994; **266**, 1591-2.
- [11] MB Zimmermann. The influence of iron status on iodine utilization and thyroid function. *Annu. Rev. Nutr.* 2006; **26**, 367-89.
- [12] S Toyokuni, Iron-induced carcinogenesis: The role of redox regulation. *Free Radical Biol. Med.* 1996; **20**, 553-66.
- [13] JR Burdo and JR Connor. Brain iron uptake and homeostatic mechanisms: An overview. *Bio. Metals* 2003; **16**, 63-75.
- [14] E Beutler. Iron storage disease: Facts, fictions and progress. *Blood Cells Mol. Dis.* 2007; **39**, 140-7.
- [15] SK Sahoo and G Crisponi. Recent advances on iron (III) selective fluorescent probes with possible applications in bioimaging. *Molecules* 2019; **24**, 3267.
- [16] P Patil, S Sehlangia, A Patil, C Pradeep, SK Sahoo and U Patil. A new phthalimide based chemosensor for selective spectrophotometric detection of Cu(II) from aqueous medium. *Spectrochim. Acta A* 2019; **220**, 117129.
- [17] Y Upadhyay, LT Babu, P Paira, G Crisponi, SK Ashok Kumar, R Kumar and SK Sahoo. Three-in-one type fluorescent sensor based on pyrene pyridoxal cascade for the selective detection of Zn (II), hydrogen phosphate and cysteine. *Dalton Trans.* 2018; **47**, 742-9.
- [18] NB Patil, UD Patil, PA Patil, S Bothra, SK Sahoo, S Sehlangia, CP Pradeep, AA Patil and SR Patil. A fused benzothiazolo pyrimidine based chemosensor for selective optical detection of Fe<sup>3+</sup> and I<sup>-</sup> ions in aqueous media. *ChemistrySelect* 2019, **4**, 4185-9.
- [19] N Kshirsagar, R Sonawane, P Patil, J Nandre, P Sultan, S Sehlangia, CP Pradeep, Y Wang, L Chen and SK Sahoo. Fluorescent chemosensor for Al(III) based on chelation-induced fluorescence enhancement and its application in live cells imaging, *Inorg. Chim. Acta* 2020; **511**, 119805.

- [20] JS Chib, MF Stempien, JTT Cecil, GD Ruggieri and RF Nigrelli. Physiologically active substances from marine sponges IV: Heterocyclic compounds. *J. Pharma. Sci.* 1977; **66**, 1052-4.
- [21] P Job. Formation and stability of inorganic complexes in solution. *Ann. Chim. Appl.* 1928; **9**, 113-203.
- [22] SK Sahoo, D Sharma, A Moirangthem, A Kuba, R Thomas, R Kumar, A Kuwar, C Heung-Jin and A Basu. Pyridoxal derived chemosensor for chromogenic sensing of  $\text{Cu}^{2+}$  and fluorogenic sensing of  $\text{Fe}^{3+}$  in semi-aqueous medium. *J. Luminescence* 2016; **172**, 297-303.
- [23] D Das, R Alu and M Ali. Rhodamine 6G-based efficient chemosensor for trivalent metal ions ( $\text{Al}^{3+}$ ,  $\text{Cr}^{3+}$  and  $\text{Fe}^{3+}$ ) upon single excitation with applications in combinational logic circuits and memory devices. *Analyst* 2022; **147**, 471-9.
- [24] Y Upadhyay, T Anand, L TilakBabu, P Paira. SKA Kumar, R Kumar and SK Sahoo. Combined use of spectrophotometer and smartphone for the optical detection of  $\text{Fe}^{3+}$  using a vitamin  $\text{B}_6$  cofactor conjugated pyrene derivative and its application in live cells imaging, *J. Photochem.* 2018; **361**, 34-40.
- [25] O Stern and M Volmer. Über die Abklingzeit der fluoreszenz. *Phys. J.* 1919; **20**, 183-8.